Self-Cleaning, Titanium Dioxide Based, Multilayer Coating Fabricated on Polymer and Glass Surfaces

Jussi Kasanen, Mika Suvanto, Tuula T. Pakkanen

Department of Chemistry, University of Joensuu, P.O. Box 111, FIN-80101 Joensuu, Finland

ABSTRACT: A photocatalytic self-cleaning titanium dioxide (TiO_2) coating was prepared as a multilayer coating structure by the spin-coating method. Three substrate materials (two thermoplastics and one ceramic) were used: (1) high-density polyethylene (HDPE), (2) poly(vinyl chloride), and (3) borosilicate glass (BK7). The multilayer structure consisted of a polyurethane protective layer on the substrate, two layers of photocatalytic TiO_2 on the protective layer, and finally immobilized TiO_2 particles bound in a diluted polyurethane dispersion. Photocatalytically active surfaces were achieved by reactive oxygen-plasma surface etching of the fabricated coatings. The structure and prop- erties of the coating surfaces were characterized with scanning electron microscopy and contact-angle measurements. The coatings on HDPE and BK7 were rendered superhy- drophilic by an oxygen-plasma treatment. The photocata- lytic activity and self-cleaning properties of the prepared surfaces were studied with palmitic acid (model soil), the degradation of which was confirmed by contact-angle measurements and gas chromatography analysis. © 2008 Wiley Periodicals, Inc. J Appl Polym Sci 111: 2597–2606, 2009

Key words: coatings; photochemistry; polyethylene (PE); thermoplastics

INTRODUCTION

Interest in heterogeneous catalysis, particularly pho- tocatalysis, is keen and is increasing rapidly.[1–4] The most common and most heavily researched semicon- ductor photocatalyst is titanium dioxide (TiO_2), most notably because of its chemical and biological inert- ness, mechanical toughness, high photocatalytic ac- tivity, favorable redox potential, and low cost.[5–8] Applications in which TiO_2 photocatalysis can be used include self-cleaning products, air and water purification, degradation of toxic organic waste, and production of renewable energy (hydrogen).[9,10] Some commercial products, such as self-cleaning windows, are already in everyday use.[11]

High-density polyethylene (HDPE) is one of the most widely used thermoplastics in the world today, and it is manufactured in very large quantities. HDPE is processed, by blow molding or injection molding, into bottles, toys, food containers, plastic bags, and many other products.[12] Another very im- portant thermoplastic is poly(vinyl chloride) (PVC), which finds wide use in buildings and construction (>50% of all PVC), the automotive industry, and medical devices.[13] PVC has outstanding resistance to degradation and is often preferred in long-life appli- cations such as pipes[13,14] and floor coverings.[13,15–17] Recent years have seen concern about the possible health risks of PVC. There is some indication that degradation of PVC can cause asthma and allergies in indoor use.[18,19] PVC plasticized with di(2-ethyl- hexyl)phthalate can degrade if the plasticizer migrates out of the PVC, and less plasticized PVC degrades faster.[20] Di(2-ethylhexyl)phthalate-plasti- cized PVC has experienced some competition from other plastics, such as polyolefins[21] and polyolefin- based materials.[22] Also, new kinds of plasticizers have been developed and produced to ensure a healthier environment.[21]

TiO_2 thin-film coatings can be made by various techniques, including atomic layer deposition,[23,24] chemical vapor deposition,[25] chemical spray pyroly- sis,[26] electrodeposition,[27] and sol–gel dip coating. Usually, these techniques are applied to ceramic, glass, or steel substrates because high reaction tem- peratures (a few hundred degrees Celsius) are needed to obtain crystalline TiO_2.[24–28] These temper- atures are too high for the most common polymers, which would melt or even degrade under such pro- cess conditions. Moreover, the photocatalytic degra- dation of organic substances by TiO_2 sets limitations on the use of TiO_2 with polymers.[29,30] On the other hand, large specific surface areas can be achieved with well-dispersed, immobilized TiO_2 on polymer surfaces, and these kinds of products have been pro- posed for use in applications such as wastewater treatment[31,32] and self-cleaning plastic surfaces[1].

Preparation stage	Spinning [time (s)/ rotation speed (rpm)]
Diluted PU dispersion (1 : 1; protective PU)	5/800, 10/3000, 15/6000
TiO$_2$/water suspension (2 wt % TiO$_2$)	5/800, 10/2200
Diluted PU dispersion (1 : 12; PU binder)	5/4000, 10/6000, 15/9000
Palmitic acid in 1-propanol (50 mg of palmitic acid/1 mL of 1-propanol)	5/800, 10/2200

Polymer surfaces can also be protected with a barrier layer such as SiO$_2$ so that TiO$_2$ photocatalysis does not degrade the polymer matrix.[33]

Our aim was to produce and test a novel self-cleaning coating, relying on TiO$_2$ photocatalysis, for HDPE, glass, and plasticized PVC substrates. A polyurethane (PU) dispersion was applied to protect the substrate surfaces and bind the TiO$_2$ particles onto the coating surface. PVC was plasticized with a new kind of plasticizer, a mixture of glycol dibenzoates, which are more environmentally friendly than phthalates. The photocatalytic activity of the coatings was tested by the illumination of samples coated with palmitic acid with ultraviolet (UV) light, and the degradation of palmitic acid was investigated with contact-angle measurements and gas chromatography (GC) analysis.

EXPERIMENTAL

Preparation and pretreatment of the substrate materials

Plastic resins were HDPE (CG8410, Borealis, Porvoo, Finland), which is a suitable grade for extrusion coating, and PVC (S98, Dynea, Porvoo, Finland). HDPE granules were extruded with a DSM (Geleen, Netherlands) Midi 2000 extruder and injection-molded into sample disks with a DSM microinjection-molding machine. PVC powder was dry-blended with 3 wt % liquid stabilizer (Therm-Chek 7500L, Ferro, Louvain-la-Neuve, Belgium). Blending was performed with a Henschel mixer (FM 10 L, 800726, Kassel, Germany). When the temperature reached 60°C, 30 wt % plasticizer (Benzoflex 2160, Velsicol, Rosemont, IL) was added. Dry-blended PVC powder with the stabilizer and plasticizer was extruded with the DSM Midi 2000 extruder and granulated. The granules were injection-molded into sample disks with an Arburg Allrounder 270S 350-150 injection-molding machine (Lossburg, Germany). Prepared HDPE and PVC sample disks were 2.5 cm in diameter and approximately 1.5 mm thick.

Glass disks were optical-grade borosilicate glass (BK7; Casix, Inc., Fuzhou, China). The diameter of the disks was 2.5 cm, and the thickness was 3 mm. Disks were washed with an ethanol/hydrochloric acid solution (90/10%) in an ultrasonic washer for 10 min and rinsed with ion-exchanged water.

Coating of the substrate materials

All three substrate disks (HDPE, PVC, and BK7) were coated with a waterborne PU dispersion (WF 28-453, Stahl), which was diluted with ion-exchanged water in a mass ratio of 1 : 1. The PU coating was produced with a spin coater (WS-400B-6NPP-LITE, Laurell, North Wales, PA). The diluted solution (0.3 mL) was placed on the middle of the sample disks and spin-coated. The PU film was dried in an oven at 60°C for 1 h. This layer is called the protective PU coating. All spin-coater rotation speeds and rotation times related to the different stages of preparation of the photocatalytic coating are reported in Table I. The parameters were optimized by preliminary experiments before their application to the coating preparation.

Preparation of the photocatalytic coating

The photocatalytic material was nanosized TiO$_2$ powder (P25, Degussa, Sachtleben, Germany). A suspension containing 2 wt % TiO$_2$ was prepared from ion-exchanged water (Lahti, Finland) and Degussa P25 powder. The suspension was treated for 80 min in a FinnSonic m03 ultrasonic washer to prevent agglomeration of the TiO$_2$ particles and break down existing agglomerates. After ultrasonic treatment, 0.3 mL of the suspension was injected onto the middle of sample disks covered with a protective PU coating and spin-coated. The samples were dried in an oven for 10 min at 60°C. The second TiO$_2$ layer was applied in a similar way.

In the next stage of preparation, the immobilized TiO$_2$ powder was bound with a thinned PU dispersion prepared by the dilution of the PU dispersion with ion-exchanged water in a mass ratio of 1 : 12 (PU dispersion/water). The diluted solution (30 μL) was spread evenly on the sample surface and spin-coated at a high speed to force it into free spaces between the particles. Samples were dried in the oven at 60°C for 1 h. This layer is called the PU binder.

In the final stage of sample preparation, samples were etched by reactive ion etching with the use of oxygen as a reactive etching gas. Reactive ion etching was performed with a March CS 1701 reactive ion etching system (Concord, CA). The working pressure in the chamber was 80 mTorr, the oxygen flow was 20 SCCM, and the etching power was set to 200 W. Etching times were 15 and 30 s.

Photocatalytic activity studies

Etched samples were coated with palmitic acid (99%; Aldrich, Steinheim, Germany) for photocatalytic studies. Palmitic acid was dissolved in 1-propanol (reagent-grade, 99.5%; Labscan, Ltd., Dublin, Ireland) to a concentration of 50 mg/mL, and the solution was used immediately after preparation. The solution (0.3 mL) was injected onto the sample surface and spin-coated, and the solvent was left to evaporate before the UV-radiation experiments and contact-angle measurements. In the UV-radiation experiments, samples were irradiated (Black Ray B100AP, UVP, Upland, CA) for 24 h (maximum wavelength = 365 nm). The distance of the lamp from the sample surface during irradiation was 15 cm.

Water contact-angle measurements

Static water contact angles were determined with a KSV Instruments, Ltd., Cam 200 contact-angle meter with an automatic liquid dispenser (Helsinki, Finland). Contact-angle measurement is an accurate method for determining the interaction between a liquid and a solid. Experiments were carried out at room temperature with ion-exchanged water. A water droplet (4 μL) was carefully placed on the sample surface and imaged with a charged coupling device camera once a second for 30 s. The contact angle was determined mathematically through the fitting of a Young–Laplace curve around the drop. Reported apparent contact angles are averages of five contact angles determined after stabilization for 30 s.

GC analysis of palmitic acid residues

GC experiments were carried out with an HP 6890 gas chromatograph equipped with an HP 7683 automatic liquid sampler (Santa Clara, CA). The chromatograph was connected to a personal computer running Agilent ChemStation Revision A.10.01 software. The column was an HP-5 capillary column (length = 30 m, inner diameter = 0.32 mm, film thickness = 0.25 μm). After UV irradiation, the palmitic acid residue was removed from the sample disks by rinsing with hexane, and the hexane solution was collected on a glass Petri dish. Most of the solvent was allowed to evaporate, and the rest of the solution (∼ 1 mL) was transferred to the GC sample

vial (2.5 mL). The Petri dish was rinsed again with hexane, and the rinsing liquid was added to the sample vial. The solvent evaporated from the vial in an oven at 50°C. After evaporation, the Petri dish was rinsed again with hexane, and the solution was transferred to the vial, where the solvent evaporated at 50°C.

After the second evaporation, the solid residue left in the vial was palmitic acid (bp = 352°C). A trimethylsilyl ester derivative of palmitic acid was prepared with a silylating reagent (Fluka III mixture, Fluka Chemie, Buchs, Switzerland). Because of the moisture sensitivity, 300 μL of the silylating agent was added to the vials under a nitrogen atmosphere, and the vials were closed with aluminum/polytetrafluoroethylene crimp caps. Closed vials were shaken a few times and then placed in an oven at 45°C for 15 min. Stearic acid (99%; Sigma, Steinheim, Germany) was added as an internal standard (ISTD). The concentration of the ISTD solution was 25 mg of stearic acid in 1 mL of acetone. After palmitic acid was dissolved and derivatized by heating in an oven, 4 μL of the ISTD solution (100 μg of stearic acid) was added to each sample vial when the solution in the vial was still warm, and the vials were shaken thoroughly. The solution was allowed to cool to room temperature before GC analysis.

Temperature programming was used for GC. The temperatures of the injector and detector were 300 and 315°C, respectively. The sample volume injected was 5 μL, and the injection was done automatically with an autosampler. During the first step, the oven temperature was 120°C, and this was maintained for 4 min. In the second step, the heating rate of the oven was 8°C/min up to 300°C, and in the third step, the temperature was kept at 300°C for 13.5 min. Data were analyzed with Agilent ChemStation Revision A.10.01 software.

Scanning electron microscopy (SEM) analysis of surfaces

The surfaces of samples were studied with a Hitachi S4800 field emission scanning electron microscope equipped with upper and lower secondary electron detectors (Toronto, Ontario, Canada). The samples were attached to the sample holder with copper adhesive tape and coated with Pd/Pt (2 nm). An accelerating voltage of 1 kV was applied, and the general working distance was 4 mm during the SEM imaging.

RESULTS AND DISCUSSION

Development of the multilayered photocatalytic coating

A multilayered coating approach (Scheme 1) was chosen because in a one-layer coating the
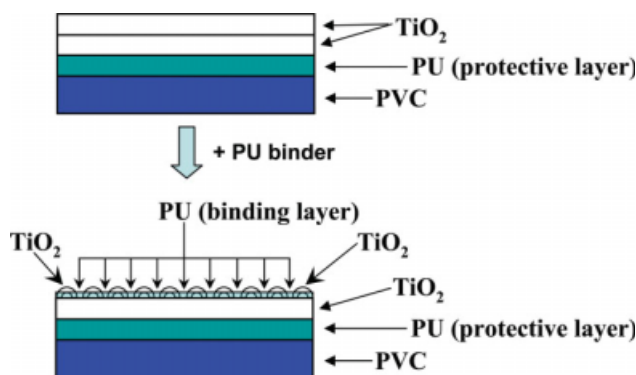
Scheme 1 Multilayered structure of a self-cleaning coating prepared on a PVC substrate. [Color figure can be viewed in the online issue, which is available at www.interscience.wiley.com.]

photocatalytic powder (TiO_2) became coated with the binding agent (PU dispersion) to such an extent that its photocatalytic activity was lost. In the multilayered structures, the primary function of the protective PU coating was to prevent direct contact of the substrate and photocatalytic TiO_2 powder. The second function was to assist with the dispersion of the photocatalytic powder. Unlike pure HDPE or PVC, the cured PU dispersion was hydrophilic, so the hydrophilic water/photocatalytic powder suspension was better dispersed on the cured PU surface than on the pure substrate. Two TiO_2 layers were needed for the whole surface to appear covered when the surface was visually examined. With just one layer, some uncoated spots were left on the surface. The fabrication of a multilayered structure on a PVC substrate is illustrated in Scheme 1.

The PU binder had to be nonviscous to be able to penetrate the spaces between TiO_2 particles. We found the PU binder in a mass ratio of 1 : 4 (PU dispersion/water) to be too viscous. The final amount of cured PU on the surface was excessive, and most of the TiO_2 particles were covered with binder, which led to photocatalytic inactivity. Thinning of the PU dispersion was therefore required (1 : 12) so that the PU binder still bound particles. A high speed in the spin coating was also important to push some PU binder between the particles by centrifugal force and cause the excess to be thrown away.

Effect of the plasma treatment

We found that, without plasma treatment, photocatalytic activity was very low or did not exist, and the superhydrophilic effect was not present. We surmised that most of the TiO_2 particles were coated with PU binder, which hindered photocatalysis, so some kind of surface treatment was required. Plasma treatment was chosen over abrasive

TABLE II
Water Contact Angles on Sample Surfaces

Sample	Substrate material	Without PU binder	With PU binder	After 15-s plasma treatment	After 30-s plasma treatment	After 15-s plasma treatment and palmitic acid	After 30-s plasma treatment and palmitic acid	24-h UV illumination (15-s plasma treatment and palmitic acid)	24-h UV illumination (30-s plasma treatment and palmitic acid)
S1	HDPE	46.7	81.3	Superhydrophilic		28.1		Superhydrophilic	
S2	HDPE		82.1		Superhydrophilic		52.2		Superhydrophilic
S3	PVC	59.5	62.0	38.9		48.0		58.7	
S4	PVC		61.9		33.4		44.0		59.9
S5	BK7	21.1	55.7	Superhydrophilic		30.4		Superhydrophilic	
S6	BK7	24.6	58.7		Superhydrophilic		52.1		Superhydrophilic

All samples consisted of a substrate (HDPE, PVC, or BK7), a protective PU coating, and two layers of TiO_2.

TABLE III
GC Integrals of UV-Illuminated Samples with Two Layers of TiO$_2$ and a Palmitic Acid Layer

Sample	Substrate material	Protective PU[a]	PU binder[b]	Plasma-treatment time (s)[c]	24-h UV[d]	Integrals of trimethylsilyl ester of palmitic acid	Integrals of trimethylsilyl ester of stearic acid (ISTD)
S1	HDPE	+	+	15	+	53.1	516.2
S2	HDPE	+	+	30	+	57.5	499.1
S3	PVC	+	+	15	+	125.5	512.5
S4	PVC	+	+	30	+	291.7	501.7
S5	BK7	+	+	15	+	52.4	498.7
S6	BK7	+	+	30	+	33.1	489.6
S7	BK7	−	−	−	+	89.5	509.3
S8	BK7	−	−	−	+	52.6	520.4
S9	HDPE	+	+	−	−	984.6	533.9
S10	PVC	+	+	−	−	656.1	537.7
S11	HDPE	+	+	−	+	845.7	546.5
S12	PVC	+	+	−	+	486.3	534.5

Samples S9 and S10 were references without oxygen plasma treatment and UV illumination.
[a] + = sample with a PU layer; − = sample without a PU layer.
[b] + = sample with a binder; − = sample without a binder.
[c] − = sample with no plasma treatment.
[d] + = sample with UV illumination; − = sample without UV illumination.

mechanical treatment because plasma treatment was expected to offer a more uniform end result. Treatments were kept relatively short, and the etching power was low so that only PU binder on the outer surface would be etched and more TiO$_2$ particles would be exposed. As can be seen from the contact-angle and GC results, the oxygen-plasma treatment was highly effective (Tables II and III).

Study of the photocatalytic degradation of palmitic acid

The photocatalytic degradation of palmitic acid was studied with contact-angle measurements and GC analysis.

Contact angles on UV-illuminated surfaces

Table II shows the average contact angles for HDPE, PVC, and BK7 samples (S1–S6). All samples consisted of a substrate (HDPE, PVC, or BK7), a protective PU coating, and two layers of TiO$_2$. Figure 1 illustrates the behavior of a water droplet on the HDPE surface under different conditions. As shown in Table II, without PU binder, contact angles on HDPE, PVC, and BK7 samples were 47 [see also Fig. 1(A)], 60, and 23°, respectively (the contact angle was ∼ 100° for pure HDPE, ∼ 65° for PVC with a plasticizer, and ∼ 31° for BK7). Clearly, without the PU binder, TiO$_2$ layers were dominant.

With the PU binder added, contact angles on HDPE [see also Fig. 1(B)] and BK7 samples rose noticeably (by over 30°), whereas the contact angle on the PVC sample rose just slightly (∼ 2°). The PU binder was now dominant, and as indicated in our previous experiments, oxygen-plasma treatment became necessary because there was no superhydrophilic effect when the samples were UV-irradiated without preceding plasma treatment.

After oxygen-plasma treatment, the HDPE [Fig. 1(C)] and BK7 samples became superhydrophilic (contact angle ∼ 0°). Oxygen-plasma treatment is known to produce hydrophilic groups, such as nonstoichiometric TiO$_x$, on the surface of TiO$_2$.[34] It has also been shown that oxygen-plasma treatment adds polar groups, such as hydroxyl groups, to the PU surface.[35] It is possible, therefore, that after oxygen-plasma treatment, the PU binder between TiO$_2$ particles contributed to the superhydrophilic effect. These polar groups on the PU binder surface interacted with water, leading to a lower contact angle.

The contact angle of the PVC samples dropped sharply from 62 to 33°, but superhydrophilicity was not achieved. This could have been due to the plasticizers in the PVC or to inadequate oxygen-plasma etching of the PU binder. Some of the plasticizer could have migrated to the PVC surface by diffusion when the protective PU coating was applied and could have mixed with the liquid PU dispersion, partially embedding the TiO$_2$ particles. The superhydrophilic effect was not observed, and the photocatalytic activity of the PVC samples was significantly reduced.

After the application of palmitic acid to the plasma-treated sample surface, the contact angles of all samples rose. Superhydrophilicity of the HDPE
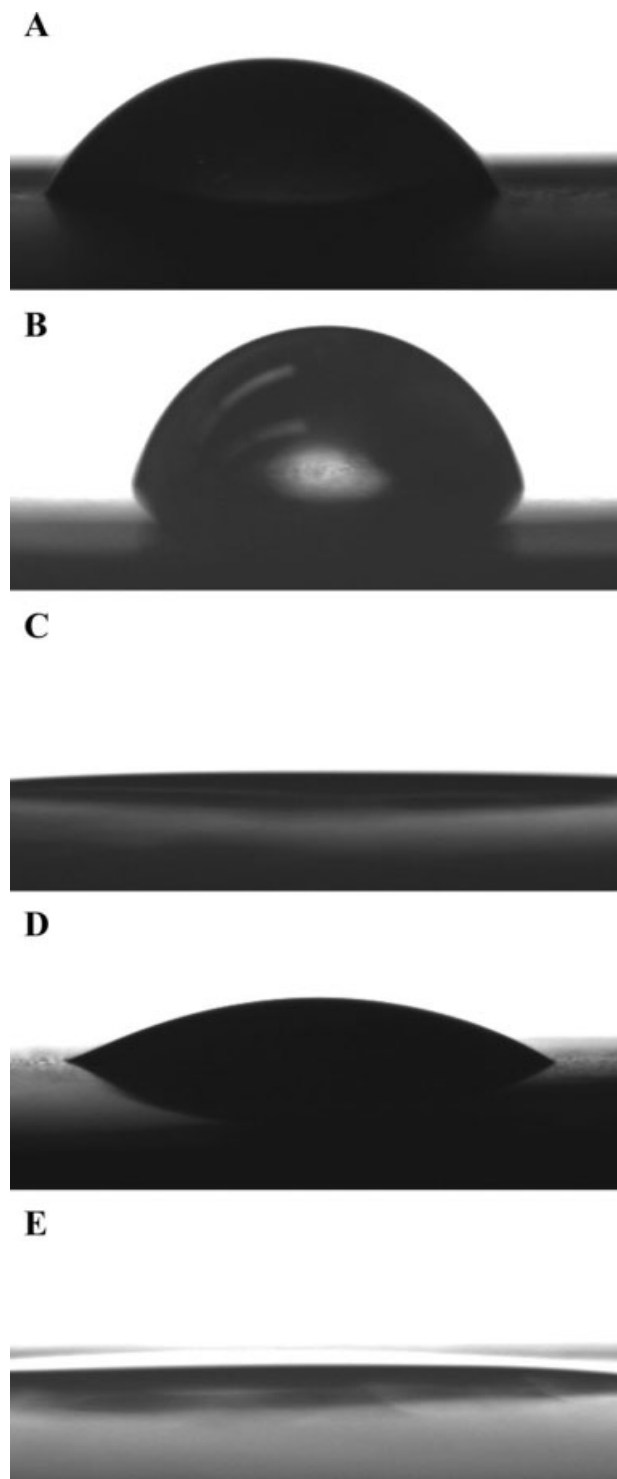
Figure 1 Water contact angles on HDPE samples at different stages of fabrication. The basic sample consisted of a substrate (HDPE), a protective PU coating, and two layers of TiO₂. The images show a sample (A) without a PU binder, (B) with a PU binder, (C) after a 15-s plasma treatment, (D) after the addition of palmitic acid to the surface, and (E) after 24-h UV illumination of the coating with palmitic acid.

[Fig. 1(D)] and BK7 samples was lost, and their contact angles leveled out to about 30°. Contact angles of the PVC samples rose by roughly 10° with respect to the oxygen-plasma-treated samples. In all cases, the addition of palmitic acid caused an increase in the contact angle versus the plasma-treated surface.

After the UV-irradiation experiments, the surfaces of the HDPE [Fig. 1(E)] and BK7 samples became superhydrophilic, but surprisingly, the contact angle on the PVC surface increased. We can assume that the superhydrophilicity of the HDPE and BK7 samples was due to the photocatalytic degradation of palmitic acid induced by UV irradiation. In the case of the PVC samples, migration of plasticizers may have caused the increase in the contact angles, and the plasticizers may also have inhibited the photocatalytic degradation of palmitic acid.

We used BK7/TiO₂ samples as references. The reference samples were prepared without a protective PU coating or PU binder, so only two layers of a TiO₂/water suspension (2 wt % TiO₂) were spread on the cleaned glass surface, and they were dried. The contact angle of the reference sample without palmitic acid was 27°, and that of the sample with palmitic acid was 97°. The activity of the TiO₂ powder was tested by illumination of the reference samples with UV light: the sample without palmitic acid for 3 h and the sample with palmitic acid for 24 h. In both cases, the contact angle dropped to 0°. The emergence of the superhydrophilic effect in the sample with palmitic acid suggests that the palmitic acid degraded, at least for the most part. Because contact-angle measurement is an indirect method, the degradation of palmitic acid was further investigated with GC analysis.

Study of palmitic acid degradation by GC

Palmitic acid residues in UV-illuminated samples were measured with GC and compared with those of reference samples that were not illuminated. GC is a highly sensitive method, allowing very small residues to be determined and the degree of degradation of palmitic acid to be estimated. The compound that was determined quantitatively was the trimethylsilyl ester derivative of palmitic acid, rather than palmitic acid itself, which has a high boiling point. Palmitic acid reacted quantitatively with the silylating agent, so the actual amount of palmitic acid on the sample surfaces could be calculated from GC integrals. Sample compositions and integrals for the palmitic acid and stearic acid (ISTD) derivatives are reported in Table III, and the residual amounts of palmitic acid in UV-illuminated samples versus those in nonilluminated samples are reported in Table IV.

TABLE IV
Amount of Palmitic Acid on Sample Surfaces After UV Illumination and on Nonilluminated Reference Sample (S9 and S10) Surfaces

Sample	Substrate	Plasma-treatment time (s)[a]	24-h UV[b]	Amount of palmitic acid in sample (µg)	Palmitic acid residue remaining with respect to reference sample (%)
S1	HDPE	15	+	10.29	5.6 (S1/S9)
S2	HDPE	30	+	11.52	6.2 (S2/S9)
S3	PVC	15	+	24.49	20.1 (S3/S10)
S4	PVC	30	+	58.15	47.7 (S4/S10)
S5	BK7	15	+	10.50	
S6	BK7	30	+	6.76	
S7	BK7	−	+	17.58	
S8	BK7	−	+	10.11	
S9	HDPE	−	−	184.44	
S10	PVC	−	−	122.02	
S11	HDPE	−	+	154.76	83.9 (S11/S9)
S12	PVC	−	+	90.99	74.6 (S12/S10)

[a] − = sample with no plasma treatment.
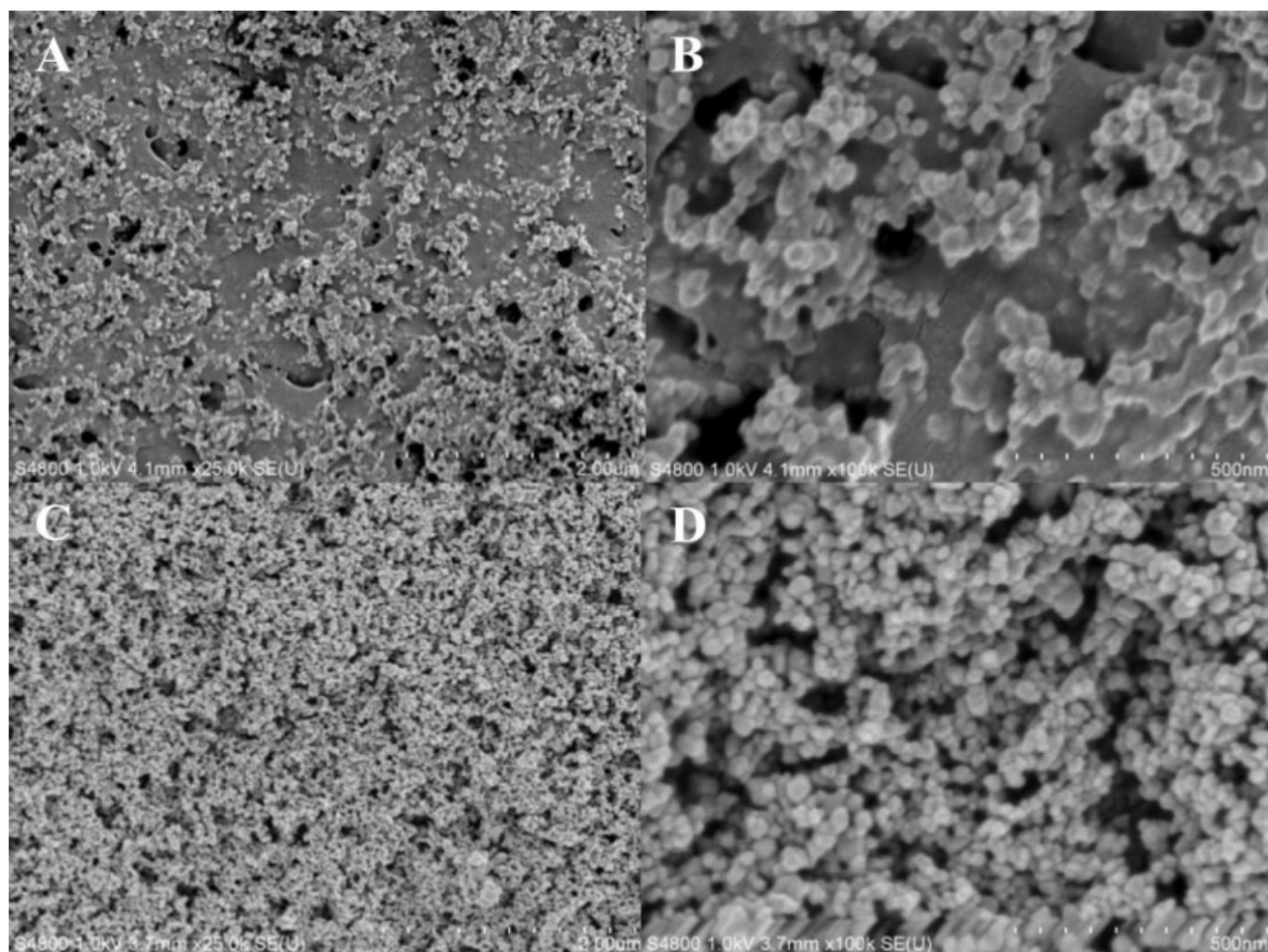[b] + = sample with UV illumination; − = sample without UV illumination.

Figure 2 SEM images of HDPE samples: (A,B) without plasma treatment (S11) and (C,D) after a 15-s plasma treatment (S1). The magnifications are (A,C) 25,000× and (B,D) 100,000×.
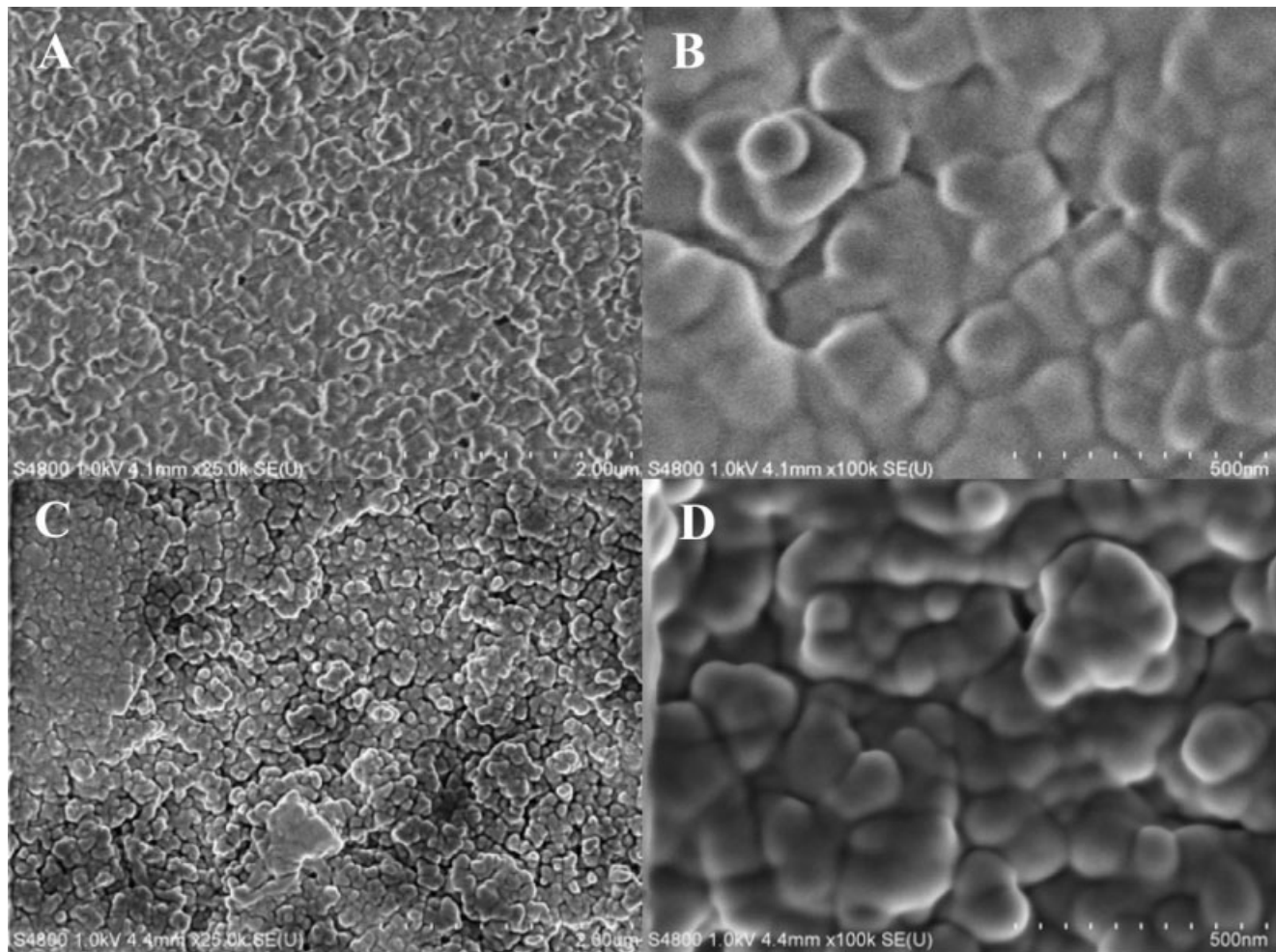
Figure 3 SEM images of PVC samples: (A,B) without plasma treatment (S12) and (C,D) after 30-s plasma treatment (S4). The magnifications are (A,C) 25,000× and (B,D) 100,000×.

The UV-illuminated BK7 glass/TiO_2 samples (S7 and S8 in Table III) were used as universal references for the evaluation of the photocatalytic activity of TiO_2 on other substrate materials. There are no additional substances in glass that can affect photocatalysis, unlike polymer substrates, which can contain additives. From Table III, we can see that the GC integral values (trimethylsilyl ester of palmitic acid) of the UV-illuminated HDPE (S1 and S2) and BK7 samples (S5 and S6) were on the same level as those of the reference samples without a protective PU coating or PU binder (S7 and S8), but the integral values of the PVC samples (S3 and S4) were much higher. This was probably due to the catalytic inhibition induced by the migration of plasticizers from PVC to the surface of TiO_2 particles. Additional signals from PVC samples appeared in GC chromatograms at high temperatures. The pure stabilizer and plasticizers were analyzed by GC for reference purposes, and three strong signals for the PVC samples (S3, S4, S10, and S12) at retention times of 21.5,

22.5, and 25.3 min were confirmed to originate from the plasticizers.

In Table III, the integral of palmitic acid is not zero for any sample (S1–S8). Possible reasons for nonzero values are deactivation of the catalyst, incomplete TiO_2 coverage, and spreading of some of the palmitic acid, with the solvent, on the sides of the sample disk during the spin coating. Because no signals from intermediate products of palmitic acid (carboxylic acids, linear alkanes, etc.)[36] were found in gas chromatograms, we can assume that the TiO_2 coverage was complete and the palmitic acid on the TiO_2 surface degraded completely. For the same reason, deactivation of the TiO_2 catalyst during the photocatalysis was therefore improbable. More likely, palmitic acid that had spread onto the sides of samples was rinsed off with the n-hexane, and that was the source of the weak palmitic acid signal observed in GC chromatograms of all the samples.

From Table IV, we can see that in the case of HDPE samples (S1 and S2), there is only ∼ 6% of

palmitic acid left when UV-illuminated samples are compared to the nonilluminated HDPE sample (S9). When PVC samples are compared (S3 and S4 to S10), it can be seen that the photocatalytic degradation of palmitic acid is not as effective as in the case of HDPE, and this can be related to photocatalytic inhibition caused by PVC plasticizers.

GC results in Table IV indicate that UV illumination of samples without oxygen-plasma treatment can induce the degradation of palmitic acid (S11/S9 and S12/S10), but the degradation was significantly lower in comparison with the samples that were plasma-treated. It can be concluded that the oxygen-plasma treatment of the PU binder was effective and contributed to palmitic acid degradation on both polymer substrates. However, longer oxygen-plasma-treatment times were not found to enhance the photocatalytic degradation of palmitic acid (S1 versus S2 and S3 versus S4).

SEM analysis of surfaces

The TiO$_2$ coatings were examined with SEM to discover the effect of oxygen-plasma etching on the amount of the PU binder. The SEM characterization was performed for HDPE, PVC, and BK7 samples after the photocatalytic studies.

Figures 2(A,B) (S11) and 3(A,B) (S12) show the HDPE and PVC samples without oxygen-plasma etching. Without etching, most of the TiO$_2$ particles were embedded in the PU binder [Figs. 2(A,B) and 3(A,B)]. SEM images after oxygen-plasma etching of HDPE (S1) and PVC (S4) sample surfaces are presented in Figures 2(C,D) and 3(C,D). After a 15-s plasma treatment, most of the PU binder was etched from the HDPE sample [Fig. 2(C,D)]; after a 30-s plasma treatment of the PVC sample, however, very little of the PU binder was etched away [Fig. 3(C,D)]. Most of the TiO$_2$ particles on PVC were still embedded in the PU binder. Clearly, the substrate material has an effect on the etching efficiency, and etching times must be optimized. The migration of plasticizers was not, therefore, the only reason for the high contact angle of water on the PVC samples because most of the PU binder was left on the surface after plasma treatment [Fig. 3(C)], and the PU binder also affected the contact angle. From the contact-angle and GC results, it is clear that, in the case of the PVC samples, excessive PU binder residue affected both the contact angle and photocatalytic efficiency.

According to the SEM experiments, BK7 lies between HDPE and PVC in terms of etching efficiency. A plasma treatment of 30 s seemed to be too long for BK7 because most of the PU binder was etched away, but a 15-s treatment left some PU binder between the TiO$_2$ particles.

CONCLUSIONS

Self-cleaning surfaces relying on TiO$_2$ photocatalysis were successfully prepared by the deposition of a multilayer coating structure. The photocatalyst was bound with PU polymer to (1) fix particles on the surface and (2) improve the mechanical resistance of the TiO$_2$ layer. Some oxygen-plasma etching was necessary to remove excess PU binder so that TiO$_2$ particles would be sufficiently exposed and the surface would become photocatalytically active. The superhydrophilic effect was observed after plasma treatment and UV illumination in the case of HDPE and BK7 samples, but the effect was not achieved with PVC samples because of the inadequacy of the plasma treatment and the migration of plasticizers to the surface of the coating. The presence of the plasticizer was confirmed in GC experiments, and it may be that the plasticizer reduced the etching efficiency of the oxygen-plasma treatment. SEM images suggested that the effect of the plasma treatment depends on the substrate material, and optimization of the etching time is required for each substrate material separately so that TiO$_2$ particles are bound and the photocatalytic efficiency remains at a high level. We conclude, on the basis of these experiments, that self-cleaning surfaces can be manufactured on both polymer and glass surfaces.

References

1. Fujishima, A.; Zhang, X.; Tryk, D. A. Int J Hydrogen Energ 2007, 32, 2664.
2. Van Gerven, T.; Mul, G.; Moulijn, J.; Stankiewicz, A. Chem Eng Process 2007, 46, 781.
3. Fujishima, A.; Zhang, X. CR Chim 2006, 9, 750.
4. Mills, A.; Le Hunte, S. J Photochem Photobiol A 1997, 108, 1.
5. Carp, O.; Huisman, C. L.; Reller, A. Prog Solid State Chem 2004, 32, 33.
6. Hagfeldt, A.; Grätzel, M. Chem Rev 1995, 95, 49.
7. Linsebigler, A. L.; Lu, G.; Yates, J. T., Jr. Chem Rev 1995, 95, 735.
8. Brunella, M. F.; Diamanti, M. V.; Pedeferri, M. P.; Di Fonzo, F.; Casari, C. S.; Li Bassi, A. Thin Solid Films 2007, 515, 6309.
9. Hoffmann, M. R.; Martin, S. T.; Choi, W.; Bahnemann, D. W. Chem Rev 1995, 95, 69.
10. Fujishima, A.; Hashimoto, K.; Watanabe, T. TiO$_2$ Photocatalysis: Fundamentals and Applications, 1st ed.; BKC: Tokyo, 1999; Chapter 1.
11. Mills, A.; Lee, S.-K. J Photochem Photobiol A 2002, 152, 233.
12. Handbook of Plastics, Elastomers & Composites, 4th ed.; Harper, C. A., Ed.; McGraw-Hill: New York, 2002; p 40.
13. Menges, G. Pure Appl Chem 1996, 68, 1809.
14. Davis, P.; Burn, S.; Moglia, M.; Gould, S. Reliab Eng Syst Safe 2007, 92, 1258.
15. Pritz, T. Appl Acoust 1996, 49, 179.
16. Ito, M.; Nagai, K. Polym Degrad Stab 2007, 92, 1692.
17. Kuisma, R.; Redsven, I.; Pesonen-Leinonen, E.; Sjöberg, A.-M.; Hautala, M. Wear 2005, 258, 826.

18. Tuomainen, A.; Seuri, M.; Sieppi, A. Int Arch Occupat Environ Health 2004, 77, 222.
19. Bornehag, C.-G.; Lundgren, B.; Weschler, C. J.; Sigsgaard, T.; Hagerhed-Engman, L.; Sundell, J. Environ Health Perspect 2005, 113, 1399.
20. Shashoua, Y. R. Polym Degrad Stab 2003, 81, 29.
21. Rahman, M.; Brazel, C. S. Prog Polym Sci 2004, 29, 1223.
22. Bani-Hani, M.; Banu, D.; Campanelli, J.; Feldman, D. J Appl Polym Sci 1999, 74, 1156.
23. Aarik, J.; Aidla, A.; Uustare, T.; Ritala, M.; Leskelä, M. Appl Surf Sci 2000, 161, 385.
24. Aarik, J.; Aidla, A.; Mändar, H.; Uustare, T. Appl Surf Sci 2001, 172, 148.
25. Bessergenev, V. G.; Pereira, R. J. F.; Mateus, M. C.; Khmelinskii, I. V.; Vasconcelos, D. A.; Nicula, R.; Burkel, E.; Botelho do Rego, A. M.; Saprykin, A. I. Thin Solid Films 2006, 503, 29.
26. Conde-Gallardo, A.; Guerrero, M.; Castillo, N.; Soto, A. B.; Fragoso, R.; Cabanas-Moreno, J. G. Thin Solid Films 2005, 473, 68.
27. Karuppuchamy, S.; Jeong, J. M.; Amalnerkar, D. P.; Minoura, H. Vacuum 2006, 80, 494.
28. Sonawane, R. S.; Hedge, S. G.; Dongare, M. K. Mater Chem Phys 2002, 77, 744.
29. Ohtani, B.; Adzuma, S.; Nishimoto, S.-I.; Kagiya, T. Polym Degrad Stab 1992, 35, 53.
30. Cho, S.; Choi, W. Photochem Photobiol A 2001, 143, 221.
31. Dhananjeyan, M. R.; Kiwi, J.; Thampi, R. Chem Commun 2000, 15, 1443.
32. Yuan, G.; Wei, Y.; Baohua, C.; Yongxiang, M.; Hulin, L. Rare Met 2003, 22, 137.
33. Schmidt, H.; Naumann, M.; Müller, T. S.; Akarsu, M. Thin Solid Films 2006, 502, 132.
34. Jung, C.-K.; Bae, I.-S.; Song, Y.-H.; Boo, J.-H. Surf Coat Technol 2005, 200, 1320.
35. Sanchis, M. R.; Calvo, O.; Fenollar, O.; Garcia, D.; Balart, R. J Appl Polym Sci 2007, 105, 1077.
36. Roméas, V.; Pichat, P.; Guillard, C.; Chopin, T.; Lehaut, C. New J Chem 1999, 23, 365.